Chem. Mater. **1993,** *5,* 54–60

Characterization of Cu–CuTCNQ–M Devices Using Scanning Electron Microscopy and Scanning Tunneling Microscopy

J. J. Hoagland, X. D. Wang, and K. W. Hipps*

Department of Chemistry and Materials Science Program, Washington State University,
Pullman, Washington 99164-4630

Received August 7, 1992. Revised Manuscript Received October 23, 1992

Scanning electron microscopy and scanning tunneling microscopy are used to determine the morphology of CuTCNQ films made using solution phase and vapor phase spontaneous formation methods. Values of film thickness range from 0.1–20 μm. All the films, irrespective of their method of preparation, display roughness on the order of their thickness. On the other hand, the morphology of these films varied significantly with preparation procedure. Resistance data from Cu–CuTCNQ–M devices (where M = Cu, Al, or Cr) are reported as a function of timed exposure of the freshly made devices to various gasses. Only devices having a thin Al top metal show significant resistance (>100 Ω for a 1 mm^2 junction), and then only after exposure to air. We suggest that the electrical switching phenomena often reported in Cu–CuTCNQ–Al structures cannot be understood without considering the interfacial interaction between the CuTCNQ film and the top metal.

Introduction

Since the discovery that films of copper 7,7,8,8-tetracyanoquinodimethane (CuTCNQ)[1] exhibit a bistable switching phenomena, there have been many attempts to determine the switching mechanism.[2–17] This switching phenomena can be observed by sandwiching films of CuTCNQ (about 1 μm thick) between a copper and an aluminum electrode and then applying a potential of sufficient strength.[1–5,13,14] The mechanism by which this phenomena occurs is still not clear. An often-quoted mechanism proposed by Potember[2–5] states that when an electric field of sufficient strength (independent of direction) is applied, the film will switch to the low resistance state (a few hundred ohms). When the direction of the field is reversed, Potember reports that the material will return to its high impedance state (megohms).[1–5] Potember believes that the observed switching is a bulk property of CuTCNQ and depends only upon the applied electric field through the following process:

$$\underset{\text{high impedance}}{(Cu^{+}TCNQ^{-})_n} \Leftrightarrow Cu^{0}_{x} + \underset{\text{low impedance}}{TCNQ^{0}_{x}} + (Cu^{+}TCNQ^{-})_{n-x} \qquad (1)$$

Although several groups have observed the switching phenomena, their results differ and do not necessarily support the mechanism proposed by Potember. That is, the critical field strength required to cause switching and the resistances obtained for the high and low impedance states differ significantly. Some studies suggest that the phenomena may not be a bulk property, but an interfacial phenomena involving the metal electrodes.[13,14] Potember reports that the threshold for switching is the same in both polarities; but, others observe marked asymmetry in the switching threshold with bias direction.[13] Sato and co-workers also report that the switching threshold does not depend on film thickness;[13] i.e., it is not readily identified as an electric field induced phenomena. Also, the resistivity of bulk CuTCNQ is only about 100 Ω cm.[15,16,18] According to the proposed mechanism, the high impedance state should only be a few ohms; but, according to most reports,[2–5,13,14] the initial junction resistance is in the region of 10^5 Ω.

To complicate the issue further, changes in state of CuTCNQ have been induced by photons[6,7,8,10,12] and by application of large voltage pulses[5,17] in the scanning tunneling microscope. While the changes produced by photons or by high voltage in the STM can apparently be reversed by heating, no one has demonstrated that these processes can be reverse by application of an electric field. Thus, it is possible that the mechanisms for the three forms of switching are all different. In our opinion, the forward process in eq 1 has been most clearly demonstrated to apply to the photon induced process wherein the reverse

---

(1) Potember, R. S.; Poehler, T. O.; Cowan, D. O. *Appl. Phys. Lett.* **1979,** *34,* 405.

(2) Potember, R. S.; Poehler, T. O.; Cowan, D. O.; Brant, P.; Carter, F. L. Bloch, A. N. *Chem. Scr.* **1980,** *17,* 219.

(3) Potember, R. S.; Poehler, T. O.; Cowan, D. O.; Carter, F. L.; Brant, P. *Molecular Electronic Devices*; Carter, Ed.; Marcel Deckker; New York, 1982; p 73.

(4) Potember, R. S.; Poehler, T. C.; Hoffman, R. C.; Speck, K. R. *Molecular Electronic Devices II*; Carter, Eds.; Marcel Dekker; New York, 1987; p 91.

(5) Yamaguchi, S.; Viands, C. A.; Potember, R. S. *J. Vac. Sci. Tech.* **1991,** *B9,* 1129.

(6) Benson, R. C.; Hoffman, R. C.; Potember, R. S.; Bourkoff, E.; Poehler, T. O. *Appl. Phys. Lett.* **1983,** *42,* 855.

(7) Potember, R. S.; Hoffman, R. C.; Benson, R. C.; Poehler, T. O. *J. Phys.* **1983,** *44,* C3-1597. Poehler, T. O.; Potember, R. S.; Hoffman, R.; Benson, R. C. *Mol. Cryst. Liq. Cryst.* **1984,** *107,* 91.

(8) Hoffman, R. C.; Potember, R. S. *Appl. Opt.* **1989,** *28,* 1417.

(9) Kamitsos, E. J.; Tzinis, C. H.; Risen, W. M. *Solid State Commun.* **1982,** *42,* 561.

(10) Kamitsos, E. I.; Risen, W. M. *Solid State Commun.* **1983,** *45,* 165.

(11) Kamitsos, E. I.; Risen, W. M. *J. Chem. Phys.* **1983,** *79,* 5808.

(12) Kamitsos, E. I.; Risen, W. M. *Mol. Cryst. Liq. Cryst.* **1986,** *134,* 31.

(13) Sato, C.; Wakamatsu, S.; Tadokoro, K.; Ishii, K. *J. Appl. Phys.* **1990,** *68,* 6535.

(14) Duan, H.; Mays, M. D.; Cowan, D. O.; Kruger, J. *Synth. Met.* **1989,** *28,* C675.

(15) Melby, L. R.; Harder, R. J.; Hertler, W. R.; Benson, R. E.; Mochel, W. E. *J. Am. Chem. Soc.* **1962,** *84,* 3374.

(16) Siemon, W. J.; Bierstedt, P. E.; Kepler, R. G. *J. Chem. Phys.* **1963,** *39,* 3523.

(17) Matsumoto, M.; Nishio, Y.; Tachibana, H.; Nakamura, T.; Kawabata, Y.; Samura, H.; Nagamura, T. *Chem. Soc. Jpn.* **1991,** 1021.

0897-4756/93/2805-0054$04.00/0

process can be reliably initiated by heating. In the STM "writing" case the products have not been identified, and it has not been shown that the process is reversed by applying an opposed voltage.

To better understand the properties of this interesting material and to resolve some of the questions surrounding the behavior of Cu–CuTCNQ–M devices, a multifaceted study of the structure, composition, and electronic properties of these structures is required. In the present paper, we will address the role played by CuTCNQ film morphology in determining the electronic characteristics of the completed device.

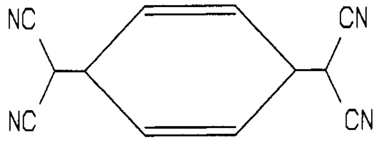

TCNQ

The CuTCNQ films used in this study were prepared by two different basic methods. The first method, employed by Potember,[1] is based on the fact that solutions of TCNQ react with copper metal by a spontaneous redox reaction that forms dark blue microcrystals of CuTCNQ on the surface of copper.[15,16,18,19] This method is the most often used, although different authors sometimes chose other concentrations of TCNQ, different solvents, various Cu substrate cleaning methods, or other reaction tempertures. We did not attempt, therefore, to make morphological measurements on films prepared at every possible point on the time, concentration, temperature, and pressure axes. Rather, we chose a limited concentration range and observed the effects of reaction time and temperature. The remainder of our CuTCNQ films were produced by sequential deposition of TCNQ and Cu under vacuum.[5,10] Cu is first deposited, followed by resistively deposited TCNQ, and the sequence is repeated. These films are then heated to increase diffusion and more rapidly form the CuTCNQ layer.

In this paper we will demonstrate that changing the growth parameters significantly changes the morphology of the resulting CuTCNQ film. These morphological changes can lead to changes in the electronic properties of the resulting Cu–CuTCNQ–metal devices. Of overriding importance is the roughness of the CuTCNQ films formed.

Experimental Section

CuTCNQ films were grown on pure Cu substrates and on Cu films resistively deposited on glass microscope slides. For the film growth experiments, substrates were made from oxygen-free high-purity copper rod. The rod was machined into disks suitable for use in scanning electron microscopy (SEM). Copper disks were polished using successive grits of emery paper down to 4/0. They were then cleaned to remove sanding particles and organics from the surface. Previous studies used several cleaning methods—we tried all of them to determine their relative merits. Thus, the copper discs were cleaned by dipping in either 1:1 HNO_3 with H_2O, 1 M H_2SO_4, or 30% HF in H_2O. The copper disks were then dried and used immediately to grow CuTCNQ films.

Solution grown CuTCNQ films used for film growth studies were made as follows. A Cu metal surface (disks of total surface area 3.5 cm^2), as prepared above, was combined with 4 mL of 0.01 M TCNQ in acetonitrile (CH_3CN) for a desired amount of time at a given temperature. This was accomplished with a two-chamber glass cell that allowed the Cu and the TCNQ solution to be sealed separately under vacuum. The cell was then heated to the desired temperature and a valve between the two cells opened so the solution and Cu could be combined. After the desired amount of time the Cu–CuTCNQ bilayer was removed and rinsed with fresh solvent and then allowed to dry. The solution was not stirred during film growth. Samples varied from 5–20 μm in thickness. Thus, up to about half the total TCNQ dose was consumed during the course of the reaction.

For the solution grown samples upon which electrical measurements were made, the bottom electrode was formed by depositing 4.1 cm × 0.1 cm × 0.5 μm (length × width × height) of Cu onto a glass substrate. Within 2 min of completing this Cu electrode, it was dipped into 25 mL of a stirred saturated solution of TCNQ and CuTCNQ in acetonitrile for 2 min. The freshly formed bilayer was then rinsed with acetonitrile. Indium solder was used to attach wires to points where electrical contact would be made upon deposition of the top metal. Then the Cu–CuTCNQ film was returned to the vacuum system and the electrical leads connected to a Fluke 8842A DMM through a vacuum electrical feedthrough. These electrical leads were used to perform four-terminal junction resistance and two-terminal top metal resistance measurements. 50–100 nm of Al, Cr, or Cu was then resistively deposited across the CuTCNQ surface to form a cross strip 1 mm wide (1 mm^2 junction area). Four terminal junction resistance and top metal strip resistance were then measured as a function of time and gas exposure. The first measurements were taken at a pressure of 4×10^{-8} Torr.

For the vapor-deposited films, 100 nm of Cu was resistively deposited under vacuum using 99.999% pure Cu evaporated from a tantalum filament. Thoroughly cleaned Corning brand microscopic glass slides were used as substrates. Then, successive layers of TCNQ and Cu were deposited until the desired film thickness was reached. The thickness of each of the layers was measured using a quartz crystal film thickness monitor. The resulting structure was then heated at 110 °C for 10 min in nitrogen. A top electrode (Al, Cu, or Cr) 1 mm wide was then deposited, forming a cross strip.

TCNQ was purchased from Aldrich and was recrystallized two times from spectroscopic grade degassed acetonitrile. The solvents used were Aldrich HPLC sure-seal acetonitrile and acetone that had been degassed. Concentrations of the TCNQ solutions ranged from 10^{-3} M to saturation (about 0.015 M). All authentic compounds were synthesized by methods reported elsewhere.[15,16,19]

Scanning electron microscopy (SEM) was done using a JEOL 6400 microscope. The accelerator voltage was 25–30 keV with a working distance of 8–12 mm. Scanning tunneling microscopy (STM) was done using a STM of our own design.[20] Images were taken in constant current mode. The tip was biased at +250 mV relative to the sample and the tunneling current was 0.3 nA. Pictures were obtained using gold coated tungsten tips.[21] The W tips were formed by electrochemical etching. Some of the STM samples were coated with 10 nm of Au to assist in imaging.

The density of TCNQ was taken as 1.315 g/cm^3.[22] The density of CuTCNQ was estimated by the flotation method to be 1.7 ± 0.1 g/cm^3. A value of 8.9 g/cm^3 was used for the density of Cu metal.

Results

We first investigated solution-grown CuTCNQ films to determine the morphology of these films under different reaction conditions. Many different spots on several

---

(18) Shields, L. *J. Chem. Soc., Faraday Trans. 2* **1985**, *81*, 1.

(19) Hertler, W. R.; Hartzler, H. D.; Acker, D. S.; Benson, R. E. *J. Am. Chem. Soc.* **1962**, *84*, 3387.

(20) Hipps, K. W.; Fried, G.; Fried, D. *Rev. Sci. Instrum.* **1990**, *61*, 1869.

(21) Fried, G.; Wang, X. D.; Hipps, K. W. To be submitted.

(22) Long, R. E.; Sparks, R. A.; Trueblood, K. N. *Acta Crystallogr.* **1965**, *18*, 932.

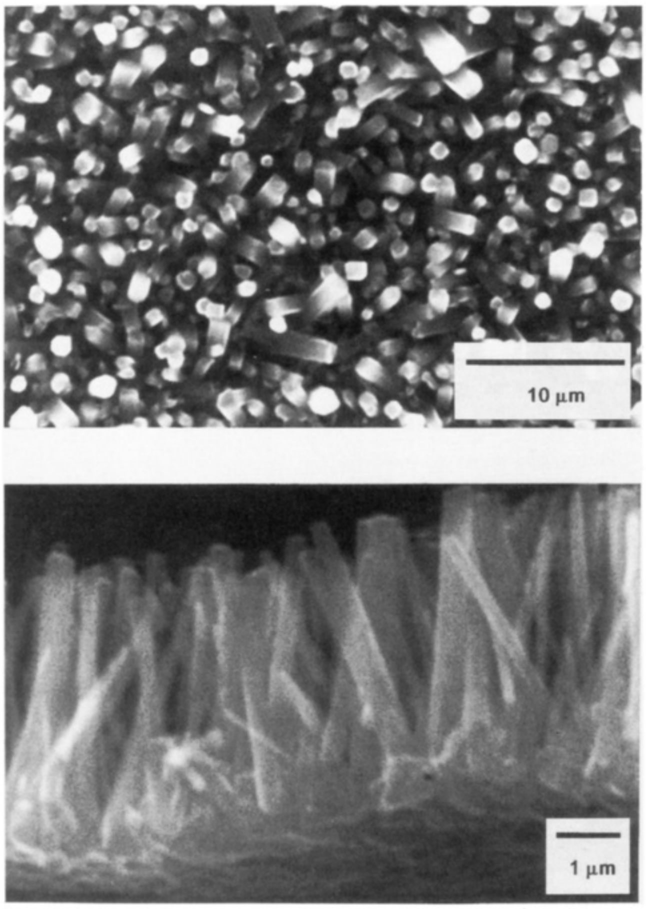

Figure 1. SEM micrographs of a CuTCNQ film formed on a copper disk that was reacted with TCNQ 0.01 M in acetonitrile for 2 min at 110 °C. Face on (upper) and side (lower) views of the same sample are shown. The side view was obtained from a segment of the film peeled from the copper substrate.

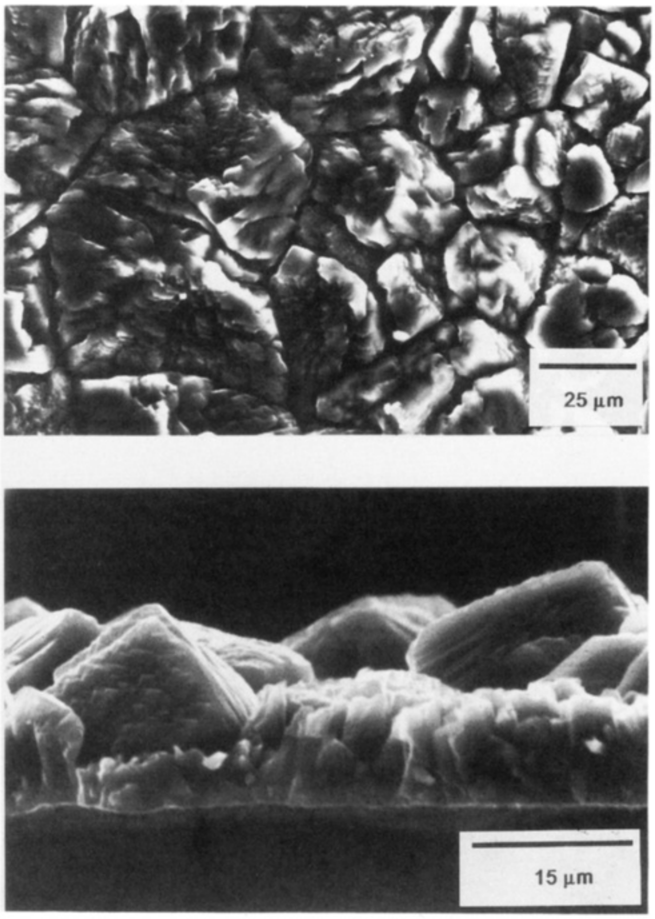

Figure 2. SEM micrographs of a CuTCNQ film formed on a copper disk that was reacted with TCNQ 0.01 M in acetonitrile for 30 min at 110 °C. Face on (upper) and side (lower) views of the same sample are shown. The structure is that of a rough mosaic. The side view was obtained from a segment of the film peeled from the surface.

similar samples were examined—the images shown here are representative of that larger set of pictures. Figure 1 shows SEM micrographs of a typical film that is formed by short reaction times at all temperatures. The structure of the film consists of long rods, about 5 μm in length and about 0.5 μm in width, oriented roughly normal to the surface and very loosely packed. The lower micrograph in Figure 1, shows that this loose packed structure extends almost to the substrate surface. This side view was obtained by peeling a flake of the film from the surface and viewing it edge on. Note that the white area below the rods is, in part, the underside of the film. What appears to be a thin amorphous layer covers the entire copper surface. Figure 2 is composed of SEM micrographs taken of a typical film produced by reaction at high temperature or by long exposure at lower temperature. The film appears to be a more tightly packed rough mosaic structure. But, the side view (the lower micrograph in Figure 2) shows that this film also has gaps that extend close to the substrate surface. Both the film thickness and mean diameter of surface structures are much larger than in the film grown for a shorter time (Figure 1).

The difference in the two morphologies probably arises from the partial solubility of CuTCNQ in the acetonitrile solvent.[23] As the CuTCNQ grows, part of it redissolves into the solvent. After a given period of time the saturation point of CuTCNQ in solution is reached, forcing CuTCNQ in solution to deposit onto the growing layer of CuTCNQ. The net effect is to cause the rods to coalesce into the mosaic structure. This process can be followed by looking at a series of different time exposures, as in Figure 3. At short times there are only rods present; but, as the time of exposure is increased from 2 to 20 min, it is apparent that the rods are slowly coalescing into the mosaic structure. While the pictures show the results of varying time at fixed temperatures, similar results were obtained by holding the exposure time constant and varying the temperature. We also note that the film seen in Figure 1 has the same morphology as the one made by Wakida[24] for use in chemical-FET applications. The structure seen in Figure 2, on the other hand, is similar in morphology and thickness to that reported by Potember.[25]

Figure 4 shows SEM micrographs obtained from Cu–CuTCNQ structures formed on a glass substrate. This sample was prepared by dipping a deposited Cu film into a stirred saturated solution of TCNQ (see experimental section). The crystallites are larger and more randomly stacked, but they retain the same general shape as those grown from 0.01 M TCNQ in actonitrile in an oxygen free environment. Note that while this film is also very rough,

---

(23) Duan, H.; Cowan, D. O.; Kruger, J. *Mater. Res. Symp. Proc.* **1990**, *173*, 165.

(24) Wakida, S.; Ujihira, Y. *Jpn. J. Appl. Phys.* **1988**, *27*, 1314.

(25) Potember, R. S.; Poehler, T. O.; Rappa, A.; Cowan, D. O.; Bloch, A. N. *Aynth. Met.* **1982**, *4*, 371.

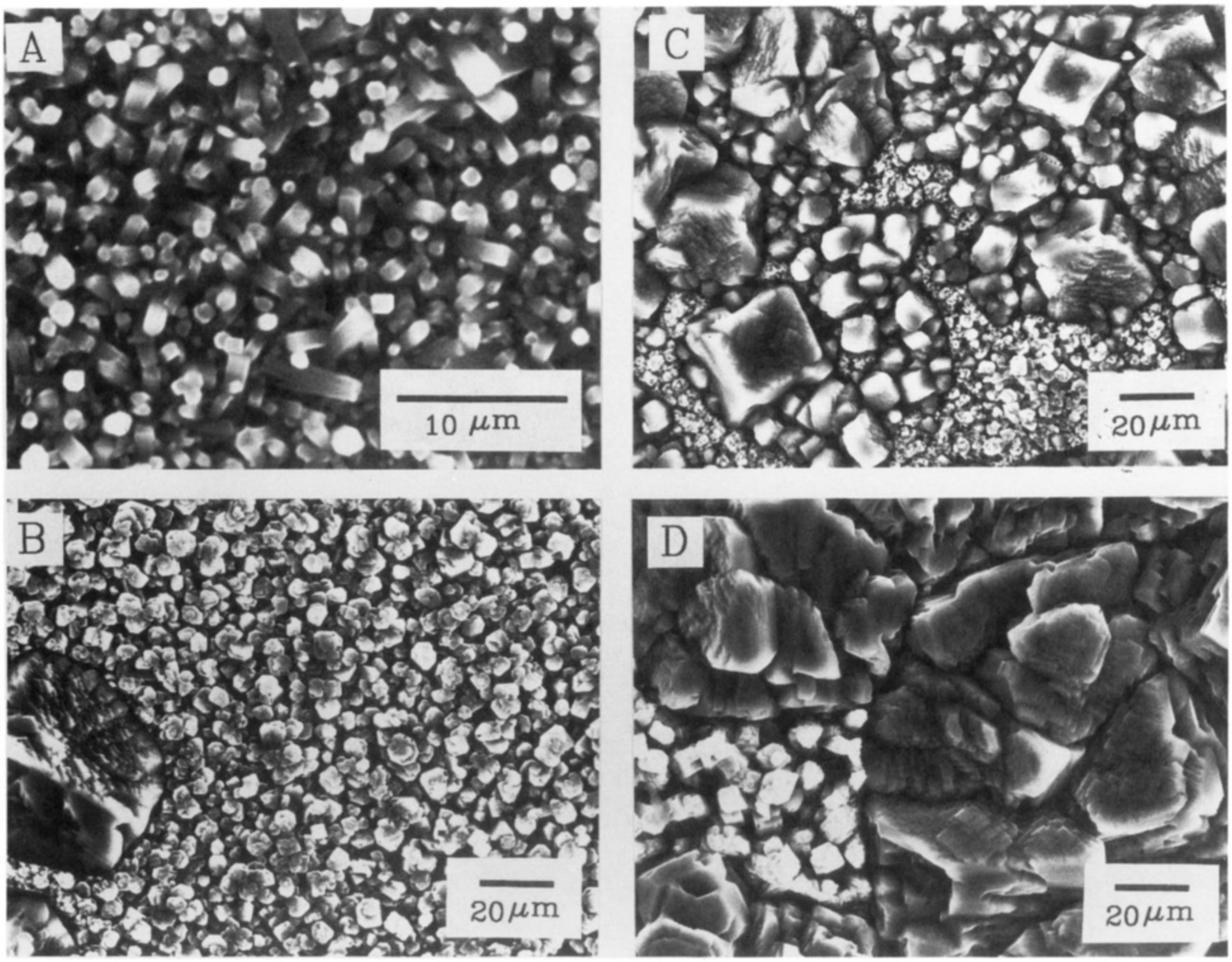

Figure 3. SEM micrographs showing the change from the rod structure to the mosaic structure. Samples made on copper disks at 110 °C, using a 0.01 M TCNQ in acetonitrile solution. In each micrograph the time has been varied by (A) 2, (B) 10, (C) 15, and (D) 20 min.

the substrate appears to be more thoroughly covered. Note also that the widths of the rods vary from about 0.5 μm to about 4 μm. These films are the solution grown films used for resistivity measurements.

Figure 5 shows an SEM image of a 75-nm-thick vapor deposited CuTCNQ film. This image shows islands of 0.5–1 μm in length. The bottom half of Figure 5 shows a STM image of the same sample. The STM image compares quite well with the SEM micrograph. From the STM image it is apparent that the valleys between the islands penetrate very deep, perhaps even reaching the substrate at some locations. Thus, the morphology of these thin deposited films is composed of islands having boundaries that occasionally penetrate to the substrate. We note here that Uyeda[26] first observed the high-resolution electron microscopy image of vapor deposited TCNQ on Al and Ag single crystals. His work emphasized the observation of single molecules of the (presumably few monolayer) films formed. The largest picture reported is only about 8 nm by 4 nm.

The resistance data obtained from our Cu–CuTCNQ–M junctions are summarized in Table I. Both solution and vapor grown films were considered. Solution grown films were limited to those having the structure of Figure 4. While it is desirable to measure those having the mosaic structure (Figure 2), those films did not adhere well to the Cu substrate, probably because the dissolution process etches them away from the Cu–CuTCNQ interface. As a result, reliable resistance and switching measurements on the mosaic structure were not obtained and are not reported.

The four terminal resistance values for several Cu–CuTCNQ–M junctions and the two terminal resistance of the top metals were measured both in vacuum and after exposure to air as a function of time. Under vacuum, none of the devices made (solution or vapor grown, using any of the top metals) showed junction resistances in excess of 15 Ω. Many junctions measured less than 1 Ω. This is completely consistent with the reported resistivity of CuTCNQ and inconsistent with past reports of the impedance of Al topped junctions.[1,2–5,13] After exposure to air, all but the Al topped junctions continue to have four-terminal resistances of less than 15 Ω. Cu–CuTCNQ–Al devices made with solution grown CuTCNQ, however, exhibited significant jumps in impedance upon exposure to air.

To better understand why only Al-coated devices that had been exposed to air showed the large junction resistances normally associated with these structures, we monitored how junction resistance changed after exposure to various gasses. As indicated in the experimental section, a given Cu–CuTCNQ–Al junction was set-up in the vacuum

---

[26] Uyeda, N.; Kobayashi, T.; Ishizuka, K.; Fujiyoshi, Y.; Inokuchi, H.; Saito, G. *Mol. Cryst. Liq. Cryst.* **1985**, *125*, 103.

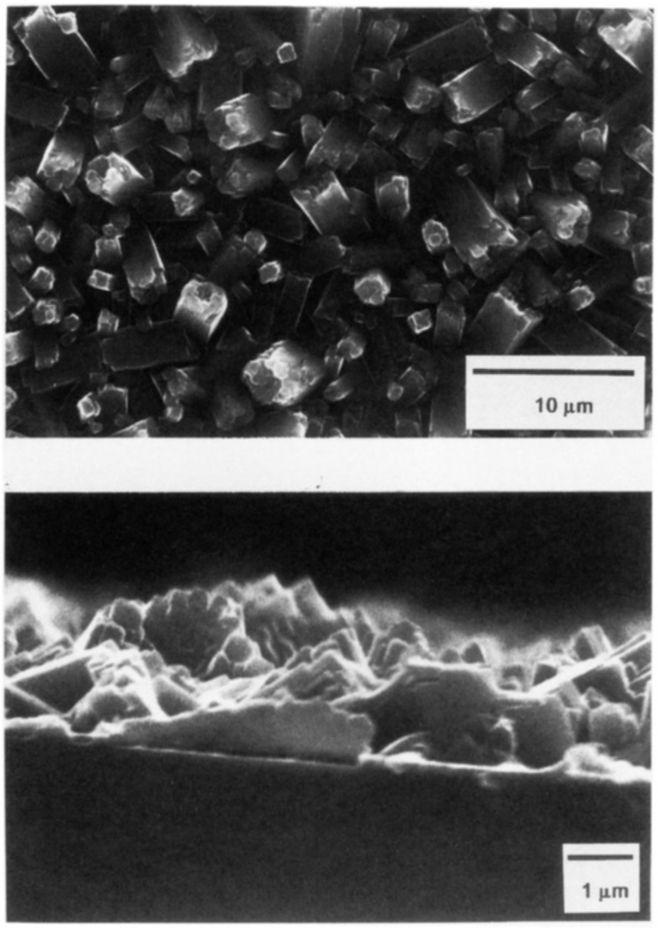

Figure 4. SEM micrograph of a 500-nm copper film reacted with a stirred saturated solution of TCNQ and CuTCNQ in acetonitrile for 2 min at room temperature. Face on (upper) and side (lower) views of the same sample are shown. The side view was obtained by fracturing the glass substrate and coating the entire sample with 10 nm of gold.

system so that the Al top electrode could be deposited and the resistances of the Al film and of the junction could be monitored in situ. We first monitored the resistance of the junction and of the metal top film while the device was under vacuum. Then, a particular gas was admitted to the chamber in order to determine its effect on the resistance of the device. Finally, the device was exposed to air. This procedure was repeated for several different devices with exposure to oxygen, nitrogen, water vapor, and vacuum during the intermediate 20-min period. Figure 6 shows the four-terminal junction resistances obtained in these experiments. For completeness, Figure 7 shows the Al top electrode strip resistances measured at the same time. Note that the top metal resistance graph is greatly expanded—the Al film resistances increase by no more than a few ohms.

Initially the junction resistances were less than 15 Ω. While under vacuum, the junctions resistance increases very slowly, probably due to residual gasses in the vacuum chamber. If nitrogen or oxygen (≈2 Torr) is admitted to the vacuum chamber, the rate of resistance increase is not significantly different than the rate in vacuum. However, if H_2O vapor (≈2 Torr) is admitted to the vacuum system, there is a significant increase in the resistance. Finally, when the samples are exposed to air, the resistance increases very quickly to about 10^4 Ω, where it stabilizes. The final resistances of the devices vary somewhat due to differences in the CuTCNQ film thickness and roughness from one sample to another. An increase in junction resistance upon exposure to water vapor occurs only for devices with Al film thickness between 30 and 100 nm. For thicker Al electrode films, the resistance of the device does not show a significant increase after exposure to air. For Al films thinner than 30 nm, the resistance of the device increases, but the resistance of the Al film increases as much as does the junction resistance. Thus, for devices with very thin Al electrodes, it is not possible to easily separate changes in electrode resistance from changes in semiconductor resistance.

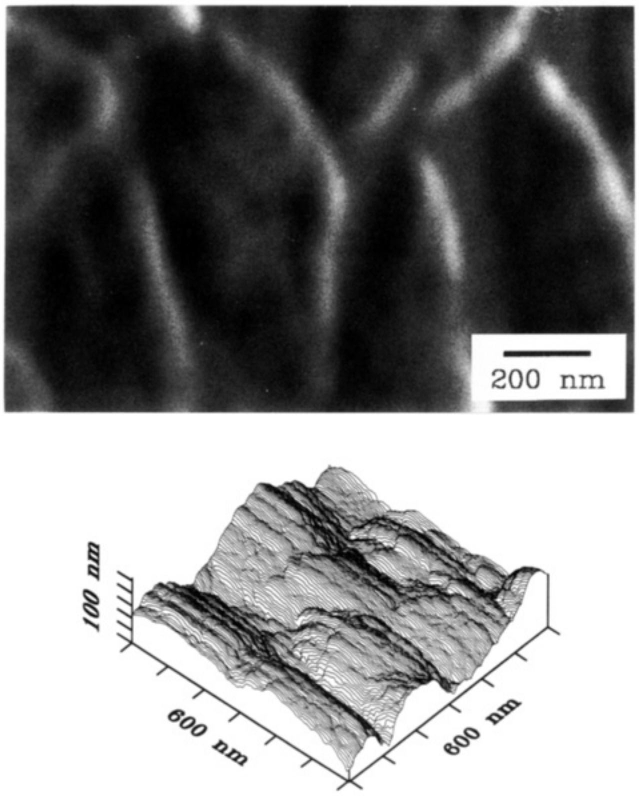

Figure 5. SEM micrograph (upper) and STM image (lower) of a vapor grown CuTCNQ film is shown. The sample was made by depositing 100 nm of copper onto a glass slide. This was followed by three repetitions of 25 nm TCNQ coated with 2 nm of Cu for a total film thickness of about 75 nm. The film was then heated under N_2 for 10 min at 110 °C. To obtain the SEM image the sample was tilted by 45°. Note that the x–y scale is the same for both SEM and STM images.

Table I. Summary of Resistance Data for 1 mm² Cu–CuTCNQ–M Junctions

	top metal			resistance (Ω)		CuTCNQ thickness (µm)
	Cr	Cu	Al	vacuum	air	
solution[a] phase	×			0.05–4	0.5–4	
		×		0.5–6	0.5–6	1–3
			×	0.05–15	10^2–10^4	
vapor[b] phase	×			0.05	0.05	
		×		0.05	0.05	0.08 ± 0.02
			×	0.05	0.05	

[a] The CuTCNQ morphology is as shown in Figure 4. [b] Single and multiple layer samples were used. The film morphology is as shown in Figure 5.

Electron micrographs of completed devices for both a vapor-phase sample and a solution-phase sample are shown in Figure 8. The upper image was obtained from a Cu–CuTCNQ (grown in saturated solution)–Al (70 nm) device. The lower image was taken of a Cu–CuTCNQ (vapor)–Au (10 nm) structure. Top metal layers of thickness less than 100 nm have no apparent effect on the image obtained

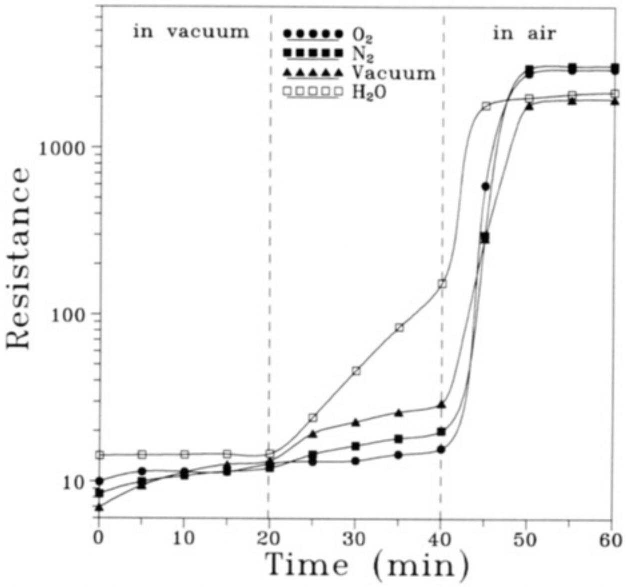

Figure 6. Graph showing resistance versus time data for Cu–CuTCNQ (solution grown)–Al films. Time zero marks the completion of Al deposition. The first 20 min show the resistance increase while the devices are under vacuum. N_2 (≈2 Torr), O_2 (≈2 Torr), or H_2O vapor (≈2 Torr) is present during the second 20 min. The vacuum system is opened to air during the last 20 min.

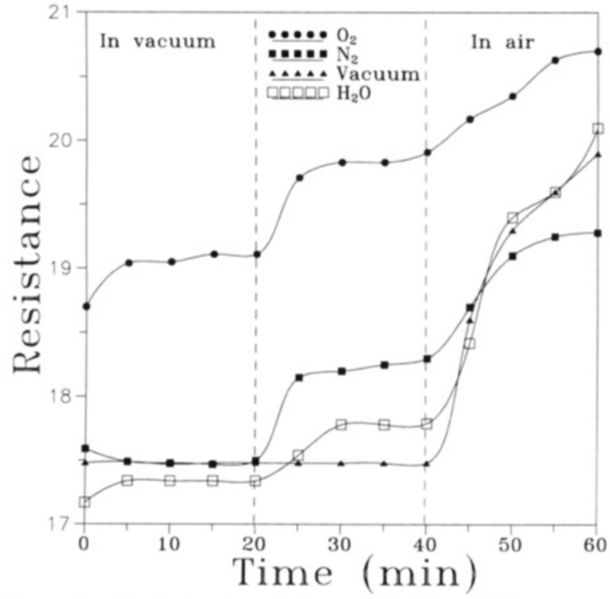

Figure 7. Graph showing Al top metal strip resistance versus time data for Cu–CuTCNQ (solution grown)–Al films. Time zero marks the completion of Al deposition. These points were taken from the same devices and at the same time as corresponding points in Figure 6.

from either the solution grown or vapor grown CuTCNQ film. Thus, for cover electrodes of the appropriate thickness to produce high junction resistance, we could not easily discern where the metal resided. For both the cover films shown in Figure 8, the CuTCNQ film corrugation is 10 times larger than their respective top metal layers. The effects produced by aluminum coating can only be seen if much thicker Al films are used (so thick that no resistance increase is observed upon exposure to air). In Figure 9 we can clearly see the result of depositing 600 nm of aluminum on a CuTCNQ film. Clusters of rods have been joined by the Al coating and Al islands are apparent along the sides of the rods. Even this very heavily overcoated device, however, cannot be viewed as a simple three-layer structure.

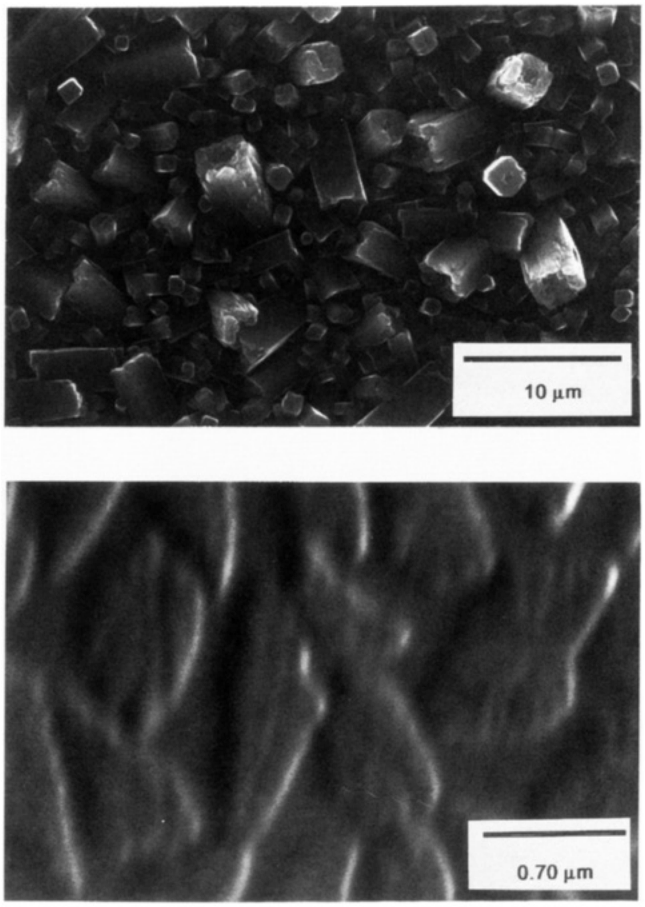

Figure 8. SEM micrographs of completed Cu–CuTCNQ–M devices. The upper micrograph shows an Al-coated (70 nm) device wherein the CuTCNQ film was grown by dipping a 500 nm thick Cu film for 2 min into a stirred acetonitrile solution saturated with TCNQ. The lower image is of a gold coated (10 nm) device wherein the CuTCNQ film was grown from vapor as follows; on a glass substrate 100 nm of Cu was deposited, followed by 25 nm TCNQ, and then 2 nm of Cu. The TCNQ and Cu depositions were repeated two more times for a total film thickness of approximately 75 nm.

The vapor grown CuTCNQ film corrugation is about equal in thickness to the Al top metal used in our conductivity measurements. Thus, we would expect 70 nm of aluminum to isolate effectively the vapor grown CuTCNQ films from the atmosphere. The same thickness of Al electrode on solution grown CuTCNQ films would be far less effective in encapsulating the CuTCNQ film.

Discussion

For the solution grown films, the SEM data indicate that there are two morphologies produced depending on the growing conditions. In both cases the films are rough with a surface corrugation of the order of the film thickness. The films grown for longer times at elevated temperatures are less rough then those grown for short times at 20 °C or 110 °C. The vapor-grown thin films produce much smoother islands but the corrugation between the islands is also similar to the thickness of the film. Independent of the growth conditions used here, all the CuTCNQ films have gaps or fissures that reach down nearly to the substrate surface.

We now can formulate an image of the Cu–CnTCNQ–Al devices that show large junction resistance. A Cu

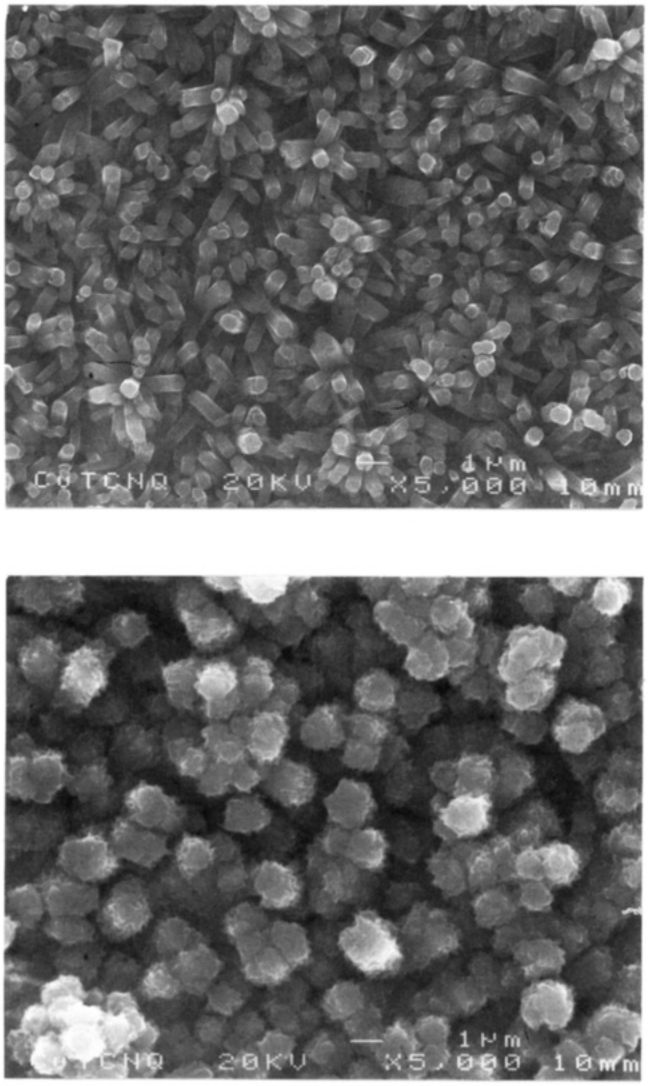

Figure 9. SEM micrographs of a single Cu–CuTCNQ film. The lower micrograph shows a portion of the film that has been coated with 600 nm of Al. The upper image is an uncoated portion of the same film. Both micrographs were taken with the same magnification and are representative of the entire coated and uncoated portions of the film, respectively. The CuTCNQ film was grown by dipping a Cu film into a stirred acetonitrile solution saturated with TCNQ.

substrate is covered by a very rough CuTCNQ layer. A thick deposited film of aluminum partially covers the CuTCNQ layer forming a very rough top electrode. At some points, the Al metal penetrates down into the fissures approaching very close to the substrate surface. Since the Al is very rough and thin, it will have a high surface area and will not be completely continuous. We might imagine islands that are connected by bridges of Al. When this Al layer is exposed to air, both its inner and outer surface will quickly oxidize to form aluminum oxide. That is, an oxide layer will grow between the CuTCNQ film and aluminum. This process affects only the outermost layer of the Al film since the Al strip resistance changes only slightly.

As Figure 6 indicates, the junction resistance initially increases very rapidly in air. After about 10 min in air the resistance stabilizes, leaving the junction at a resistance several orders of magnitude higher than before the device was exposed to air. This high impedance state might be due to one or more factors. It may result from the formation of a thin tunnel barrier (composed of AlO_x) between the top electrode and the CuTCNQ layer. It may result from chemical reaction (or doping) of CuTCNQ by water and/or O_2. This surface reaction could result in band bending at the electrode surface and an associated increase in device impedance. Also, the low initial resistance might to due to direct Cu–Al contacts through very thin Al whiskers. Oxidation of these whiskers would result in a large junction resistance increase.

The rate at which the resistance increases is dependant on the thickness of the Al films. For thick films the junction resistance goes up slowly because the film is more continuous and has fewer openings into which atmospheric gases may penetrate. Junctions made with a thin Al top electrode have Al film resistances that increase much faster because the films are more discontinuous and are more easily permeated by reactive gasses. Also, exact values for the resistance increase will depend highly on the morphology (purely rods, mosaic, or a mixture of both) of the sample. As may be seen from Figure 3, intermediate growth times will yield film structures that have a mixed morphology.

The Cu/TCNQ (vapor grown)/Al devices showed negligible four terminal resistance. Also, the resistance of these devices did not change when they were exposed to air. This can be explained by considering the STM image of these films, Figure 5. There are places where the fissures extend to the substrate, resulting in electrical shorts between top and bottom electrodes. Thus, we expect very small four-terminal resistance values for these devices in vacuum. In air, the inner surface of the Al electrode probably does not significantly oxidize because of the smaller overall corrugation of the vapor grown films. These devices have a continuous Al film that cannot be penetrated by the atmospheric gases.

The fact that only aluminum top metal devices show the high junction impedance associated with switching devices, and then only after the device is exposed to water vapor, suggests that switching is not solely a bulk property of CuTCNQ. Rather, the electrical properties of these devices depend strongly upon the interaction of the CuTCNQ and the Al/AlO_x layers. Since the electrical state of the device is heavily dependent on morphology, top metal film structure and composition, and exposure history, actual resistance and switching values can change from sample to sample or even from day to day. This fact may explain the differences in data obtained by previous studies. Future studies of these devices should take this into consideration and include true UHV conditions as part of the experimental protocol.

The bulk-property mechanism proposed by Potember for electrical switching phenomena in Cu–CuTCNQ–Al devices is not supported by our results. Rather, we agree with Ishii[13] that one must first consider interfacial interactions between the aluminum top metal, the rough CuTCNQ layer, and atmospheric gases if one is to understand the electrical properties of Cu–CuTCNQ–M devices. This does not say, however, that Potember's mechanism does not play a role. If it does, however, it is probably acting in the nanoscopic regions where the top electrode forms a deep sharp contact with the CuTCNQ film.

Acknowledgment. The authors gratefully acknowledge the support of the Environmental Protection Agency under Grant R-816329-01-0 and the National Science Foundation under Grant DMR-9201767.